The Thermomechanical Behaviour of Carbon Fibre Reinforced Polymer Exposed to Fire Conditions

T. J. Aspinall [a1], Emmajane L. Erskine [b], Derek Taylor [b], and Rory M. Hadden [a]

[a] Centre for Fire Safety Engineering, The University of Edinburgh, Edinburgh, EH9 3JL, UK
[b] Defence Science and Technology Laboratory, Dstl Porton Down, Salisbury, Wiltshire, SP4 0LQ, UK

Abstract

The vulnerability of military aircraft is an important aspect of air survivability and the effect of fire has been seen to be a critical factor in controlling platform vulnerability. Current and future trends in design and manufacture of modern aircraft has seen an increase in the use of composite materials, such as carbon fibre reinforced polymer (CFRP) materials, due to the performance benefits this offers to aero-structures. However, this presents substantial challenges in assessing their vulnerability due to the significantly different material properties between composite and metallic structures and requires an increased understanding of the thermomechanical properties and behaviour of these CFRP materials. The thermomechanical response leading to the loss of mechanical properties is governed by the effects of glass transition, thermal decomposition (pyrolysis) of the resin matrix and oxidation of the carbon fibre reinforcement. These phenomena are strongly coupled and their effect on the mechanical response of CFRP are poorly documented in the literature. This work presents the development of a method for investigating the thermomechanical properties of such materials under three-point bending subjected to different thermal exposures. Of particular interest was exploring the failure modes and the effect that the propagation of the glass transition isotherm through the sample and char oxidation on the exposed surface has on this.

Keywords: fire testing, mechanical testing, heat flux, fire safety, coupled interaction, carbon fibre reinforced polymer.

1 Introduction

Carbon Fibre Reinforced Polymers (CFRP) are used extensively in military aircraft due to their high specific strength and stiffness and excellent performance in the design and manufacture of aero-structures. Because of this, they offer an attractive alternative to using conventional materials (i.e. steel and aluminium alloys) in a wide range of applications [1]. However, this is offset by their potential low resistance and robustness to weapons effects which poses significant questions for assessing their vulnerability. One key element is their survivability to fire which can result from fuel system events following engagement by hostile effects.

In particular, the organic nature of the CFRP, and particularly the resins used, means that it will burn when exposed to certain fire conditions [2]. In addition, elevated temperatures within the material may limit the use due to a relatively low glass transition temperature (T_g). Both of these problems significantly influence the mechanical performance of CFRP at elevated temperatures.

Previous studies, which assess the fire safety of CFRP materials have been carried out using a decoupled approach whereby a material is exposed to simulated fire conditions (radiant heat flux [3]–[7], temperature [8]–[10]) and then, mechanically tested to determine residual mechanical properties. Acquiring residual mechanical properties using this approach is a well-established way of obtaining data accurately for scenarios where post-fire properties are important (e.g. after extinction), however, limitations exist if the mechanical response of a material during a fire is required. For example, important processes that CFRP materials experience during a fire, such as glass transition, resin pyrolysis, char formation and heterogeneous oxidation of the char layer and fibre reinforcement whilst under load are not captured in post-fire analysis and the true interaction due to the coupling of the thermal and mechanical processes during a fire are not well quantified. This suggests the data obtained from these tests may not be appropriate to assess

[1] Corresponding author: T. J. Aspinall, email: timothy.aspinall@ed.ac.uk

the degradation of material properties during the fire.

Therefore, a new testing approach, using apparatus that can simultaneously capture and quantify the mechanical performance of a material exposed to simulated fire conditions and characterise the mechanical performance is required. The apparatus developed to generate this data has been named the ***Thermal and Stress Inducing Device (TSID)***. In this research it has been used specifically for testing CFRP, however, practically it can be used to test any material. Emphasis will be placed on exploring the role of the failure modes due to propagation of the glass transition isotherm through the sample and oxidation of the char layer and fibre reinforcement at the exposed surface. Research into the thermomechanical behaviour of CFRP during bending is at present modest and little is known [11]. Hence, the objectives of this paper are to first describe the critical aspects of the TSID and then present a study into the thermomechanical behaviour of CFRP in three-point bending using the TSID to signify its innovation.

2 Design and Development

The apparatus developed for this study (Fig. 1 and Fig. 2), allows for a specimen to be exposed to well-defined heating through the heat flux generated by a radiant heater and also three-point bending. The fire exposure is simulated by imposing a radiant heat flux from a cone heater. The desired temperature measurements can be made by instrumenting the sample with thermocouples. The mechanical aspect is quantified using pressure from a hydraulic jack that applies a load, finally bending displacement is quantified using digital image correlation (DIC). The experiments carried out using the TSID do so with the incident heat flux applied to the sample from above and the load-displacement applied from below. The development of the TSID was carried out based on the following requirements:

1. *The ability to impose a quantifiable thermal exposure on a target surface* – This needs defining in terms of an incident heat flux rather than existing methods that mostly (but not always) quantify thermal exposure using a temperature (i.e. UTM furnace test), therefore, the size or severity of the fire and the rate of heat transfer can be directly controlled and measured.

2. *The ability to impose a range of thermal exposures* – This needs defining to replicate a wide range of prescribed and unprescribed time-temperature curves ranging from an incident heat flux necessary to ignite thin items (10 kW/m^2), up to a fire within a fully developed room fire or a large pool fire (75 - 150 kW/m^2) [12].

3. *The ability to replicate different loads a material or structure may be exposed to during a fire* – The TSID must be capable of replicating the various loads a material may undergo, either as a single component or as part of a larger structure as well as those achieved in standard mechanical testing apparatus. Currently, these are bending loads, but modification could lead to testing in pure tension or compression.

4. *Repeatability* – Repeatable calibration of the testing method (before each new test) to account for any changes in ambient conditions allowing for a high level of repeatability and good statistical confidence between tests.

1. Cone Heater: Adjustable Heat Flux and Height
2. Two-Dimensional Motion System
3. Thermally Insulated Frame
4. Load Cell
5. Hydraulics Lubrication Feed and Support Frame
6. Loading and Support Frame

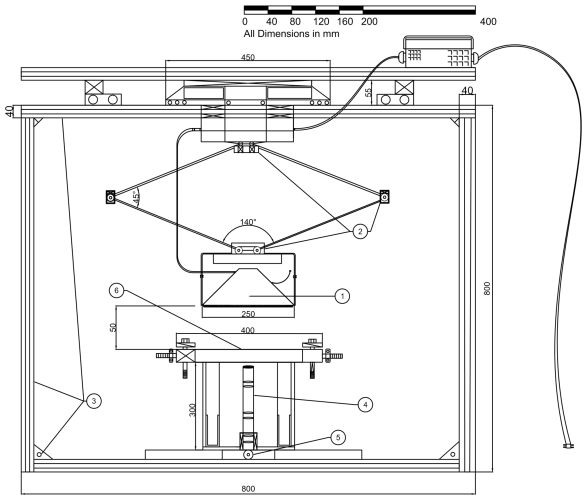

Figure *1* – The current version of the TSID (front elevation).

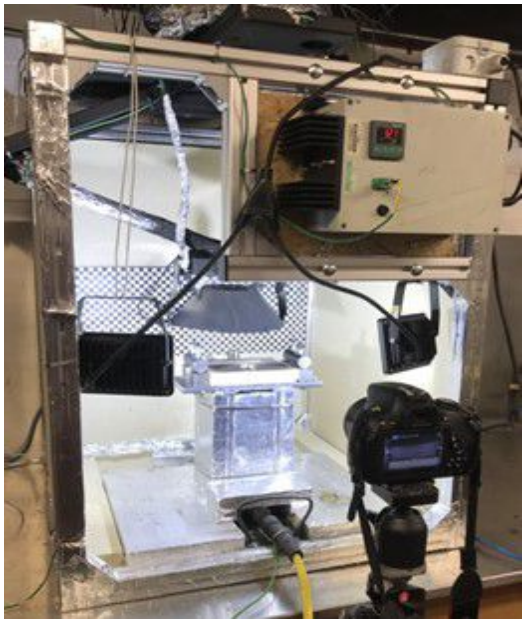

Figure *2* – A photograph of the TSID (front-left elevation).

3 Studies on Carbon Fibre Reinforced Polymers

This section illustrates the application of the TSID to evaluate the coupled thermomechanical bending behaviour of CFRP. A comprehensive review of previous studies carried out on CFRP is not the intended focus of this paper and therefore is not presented here. However, a few previous studies are discussed below to demonstrate the need for the new coupled testing approach proposed in this study.

3.1 Background

Previous experiments have investigated the thermomechanical response of a CFRP material whilst in tension [13]–[15] and in compression [14], [16], [17]. In these experiments, it was shown that the time-to-failure and failure load of a woven CFRP material is lower during a fire than it is during post-fire exper-

iments. Similarly, during compression tests, it was shown that the strength and stiffness of CFRP significantly decrease when tested at temperatures above 200 °C and buckled in a shorter time and under a smaller load during a fire than in post-fire experiments.
The post-fire bending behaviour of several FRP materials including CFRP has also been investigated [18], [19]. These tests demonstrated that the post-fire bending properties significantly reduce when tested at and above heat fluxes of 25 kW/m² and reveal that even relatively small amounts of fire damage can cause a large reduction to the materials strength and stiffness.
Still, these experiments, although contributing to the post-fire mechanical properties, do not explore the effects of the glass transition nor the depth of thermal penetration in any great level of detail because they were effectively at ambient temperature whilst under load. They, therefore, demonstrate the importance of the proposed study, and with existing literature related to the coupled thermomechanical response of CFRP during bending next to non-existent, an investigation must be carried out, hence exploring the three-point bending behaviour in a fire is the focus of this paper.

3.2 Aims of this Study on CFRP

The previous section has shown that knowledge on the bending behaviour of CFRP exposed to fire conditions is limited and that the experiments carried out to-date have largely focused on post-fire analysis. These experiments cannot capture thermomechanical processes occurring in the material whilst exposed to fire conditions and consequently are not representative of a structure (or structural component) exposed to a real fire and therefore can have huge implications on air-survivability. Therefore, this paper aims to explore the thermomechanical behaviour of a CFRP material *during a fire*. This will be achieved by capturing the coupled interaction between the propagation of the glass transition and thermal decomposition isotherms through the sample and investigate the effects this has on the mechanical properties (namely time-to-failure and displacement). By using the TSID, this can be carried out directly due to its ability to couple the fire and load whilst measuring displacement and will help to generate thermomechanical data that can feed into structural/vulnerability models.

3.3 Testing Programme

The TSID was used to explore the bending behaviour of several samples during different fire conditions. Prior to thermal exposure, a preload was applied to the testing sample at 20% of the total failure load at ambient temperature. This was done to every sample before every test. This load would stay constant throughout the test; however, it would move to adapt to any deflection of the sample to keep the load conditions consistent. The value of the 20% preload was obtained by performing tests at ambient temperature to quantify the failure load of the material under normal service conditions. The incident heat fluxes were chosen to be far enough apart from one another to demonstrate completely different thermomechanical behaviour, time-to-failure, failure mode, and displacement for relative ease of DIC analysis. Load-displacements were chosen to replicate the influence of a real "fire" on time-to-failure and bending displacement of a load-bearing CFRP component within a larger aircraft structure. Temperature distribution measurements were also taken using embedded thermocouples to allow insight into the different processes that occur within the material, this data would provide a further understanding of the heat transfer mechanisms. Rather than seeking to understand the precise failure mode contributing to the loss of bending properties or defining the fire resistance of the testing sample, this study was carried out simply to demonstrate the TSID's potential as an effective piece of apparatus by using it to evaluate the influence of four different incident heat fluxes on time-to-failure and displacement. If it could quantify the bending behaviour effectively, it could be utilised to carry out further tests to better understand the bending behaviour of other materials exposed to fire conditions. Therefore, no specific failure mode of the samples was sought, and the test was stopped when either total failure (time-to-failure) occurred, or the maximum test time was reached.

3.3.1 Details of the Testing Programme

The time-to-failure and displacement data were obtained at four different heat fluxes (10, 20, 30 and 40 kW/m²) using a 2 (±0.5) kN pre-load for a period of 300 seconds. A total of 14 tests were carried out,

3 samples at each of the heat fluxes indicated, and 2 at ambient temperature (22°C) to obtain the total ambient bending capacity of the material. Heating was from above and load-displacement from below applied at the midspan of the sample until either bending failure occurred or the sample resisted failure beyond the 300 second period of thermal exposure. The samples dimensions were 250 mm x 30 mm and comprised an exposed area of 210 mm x 30 mm located directly below the cone heater (see Fig. 3). The dimensions of all samples were identical and comprised a high-performance carbon fibre reinforced polymer for use in primary aerospace structures with a 57.42% fibre volume fraction and measuring 5 mm in thickness. Time-to-failure and displacement were recorded during each test. Failure under these conditions was defined as a deflection of 14 mm or above from the pre-load position, 14 mm was used as a reference because it was the maximum bending deflection measured at failure in ambient conditions. Temperature distribution measurements were also taken at the highest (40 kW/m²) and lowest (10 kW/m²) heat fluxes to evaluate the position of the glass transition and pyrolysis isotherm. The testing samples were held in unrestrained conditions with fixing plates at either end with the load held constant. Displacement was measured using digital image correlation (DIC). Details of the testing matrix are given in Table 1.

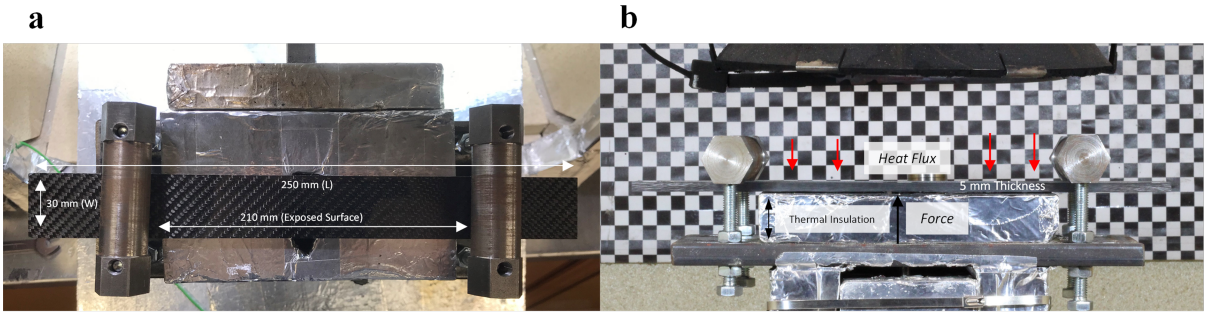

Figure *3* – Test set up in the loading frame showing (a) the sample dimensions (top view) and (b) sample relative to the cone heater (front view).

Table *1* – Experimental test matrix for bending samples tested using the TSID.

Sample No	**Heat Flux**	**Loading (Preload)**
[-]	**[kW/m²]**	[-]
1,2	0 (22°C = Room Temperature)	Total ambient capacity (10.85 kN)
3,4,5	10	20% of ambient capacity
6,7,8	20	20% of ambient capacity
9,10,11	30 (Surface heating by a turbulent wall flame)[21]	20% of ambient capacity
12,13,14	40 (Surface heating by a small laminar flame)[22]	20% of ambient capacity

**All tests were carried out with a constant pre-load of 2 (±0.5) kN, this signifies 20% of the total bending load (10.85 kN) obtained from pre-fire testing carried out using the TSID.*

4 Results and Discussion

The experiments carried out using the TSID demonstrated that coupling incident heat flux, similar to that used in flammability assessments (i.e. cone calorimeter or FPA) and load-displacement, similar to the one experienced in a bending test (i.e. Instron) can be achieved. The data generated from this study is related to the displacement and time-to-failure, with failure mode also being observed and discussed. This data is presented in Table 2. Although ignition time data was not essential for quantifying the bending behaviour of the material *per se*, it allows comparison to flammability assessments as was also noted in Table 2.

Table *2* – Experimental test matrix and results for bending samples tested using the TSID.

Sample No	**Heat Flux**	**Time to Ignition[2]**	**Time to Failure[2]**	**Maximum Displacement[2]**	**Comment**
[-]	[kW/m²]	[s]	[s]	[mm]	[-]
1,2	0 (22°C)	N/A[1]	N/A	1.5	Tested to obtain failure load at ambient temperature = 10.85 kN.
3,4,5	10 kW/m²	N/A[1]	192	14	Loss of stiffness leading to fibre kinking on the unexposed surface due to the effects of T_g (see Fig. 6a, 8a).
6,7,8	20 kW/m²	N/A[1]	128	15.5	Loss of stiffness.
9,10,11	30 kW/m²	94	103	13.8	Testing samples ignited. Partial loss of bond between the laminates (exposed surface) and localised shear due to the force from the loading nose (unexposed surface).
12,13,14	40 kW/m²	77	84	14.2	Testing sample ignited. Complete loss of bond between laminates (see Fig. 8b). Char formation (2 mm thick) on the exposed surface based on temperature measurements in Fig. 6b. The unexposed surface surpassed Tg isotherm (see Fig. 6b).

**All tests were carried out with a constant pre-load of 2 kN.*
[1] No ignition.
[2] Average taken from 3 tests.

4.1 General Observations

During the experiments, all the samples failed before the end of the 300 second period and exhibited different failure modes depending on the severity of the heat flux. At 30 and 40 kW/m², the samples ignited, burning with a turbulent flame for a few seconds before failure. Both the exposed and unexposed surfaces were quantified using DIC to obtain data on displacement and changes in sample thickness. Data relating to the displacement at the midspan of the samples can be seen in Fig. 4 as a function of time and shows that displacement occurs more slowly, over a longer period for samples tested at lower heat fluxes. It also shows that at higher heat fluxes displacement appears to coincide with sudden failure, whereas at lower heat fluxes this does not appear to be the case. At the end of the test, samples tested at higher heat fluxes (and that had ignited) had a tendency to exhibit brittle behaviour at failure, whilst at lower heat fluxes samples exhibited less brittle behaviour at failure (see Fig. 5).

After the experiments, a visual inspection of all the samples was carried out and revealed that the samples tested at higher heat fluxes, and had experienced a sudden failure during the tests, had experienced significant delamination (see Fig. 5, 30 and 40 kW/m²). These samples also displayed signs of charring of the residual resin and very small white pockets of ash, indicative of char oxidation, on the exposed surface, however, this ash cannot be seen in Fig. 5. On the unexposed surface, fibre kinking was evident, typical of glass transition, with localised shear deformation of the resin and breaks in the fibre. These observations coincide with the temperature measurements taken during the tests (see Fig. 6b) which indicate that the exposed surface (x=1 mm) had reached the pyrolysis temperature early on, however, the middle (x=2.5 mm) and unexposed (x=5 mm) surfaces had not. Generally, this behaviour provides a motive for the sudden, and at times violent failure modes experienced by samples tested at higher heat fluxes, which occur because significant anisotropic and spatial temperature variation exists across the thickness.

At lower heat fluxes (see Fig. 5, 10 and 20 kW/m²), no charring was visible and delaminations appear less evident, although, fibre kinking on the unexposed surface was still visible. The failure mode was also less sudden compared to the samples tested at higher heat fluxes and using the temperature distribution data in Fig. 6a and time-to-failure data in Fig. 9, the effects of the glass transition isotherm penetrating the entire thickness of the sample appeared to be the only process to transpire which contributed to its excessive displacement and failure.

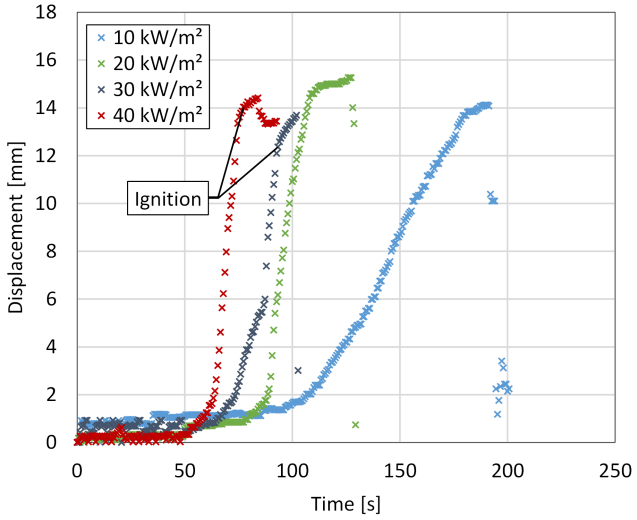

Figure *4* – The bending displacement at different heat fluxes as a function of time.

Figure *5* – Post-fire photograph of the bending samples showing left to right, 10, 20, 30 and 40 kW/m².

4.2 Details by Sample Number

The following observations can be made from the data presented in Table 2, the temperature and DIC measurements taken during the test, and comments made regarding the failure mode after the tests:

1. The failures of samples 3, 4 and 5 were attributed to the loss of stiffness caused by the propagation of the glass transition isotherm. This was characterised by fibre kinking on the exposed surface (see Fig.

5, 10 kW/m²), which is a characteristic failure mode for CFRP in compression above the T_g but below the pyrolysis isotherm [17]. The time for this isotherm (thermal wave) to reach the back of the sample was 52 secs (38 seconds for the exposed surface). This can be seen in Fig. 6a. Throughout the test no char formed as the temperatures had not reached the pyrolysis temperature (approximately 350 °C [22]), hence no ignition occurred. Therefore, it can be assumed that these samples did not undergo significant pyrolysis or char formation and the effects of the glass transition temperature represent the only significant process that contributed to failure. The displacement was slow during these tests compared to the samples at the higher heat fluxes and reached a total displacement of 14 mm in just under 200 seconds (see Fig 4). The temperature also varies with thickness, with the middle (x=1 mm) and unexposed (x= 2.5 mm) having a lower temperature than the exposed surface (x=5 mm) throughout the test. This shows that the rate of heat transfer slows considerably between the exposed and mid-thickness of the sample at low heat fluxes.

2. Samples 6 through to 8, were characterised with slight loss of bond between the laminates and very minor char formation. This char first appeared at the midspan of the sample closest to the exposed surface on the location of the loading nose and slowly throughout the test splitting down to the edges close to the fixing plates. Based on visual observation using UHD video, this did not form at a constant rate. The onset of charring (if defined by the progression of a 350°C isotherm [22]) occurred approximately 92 seconds from the onset of heating according to the in-depth temperature measurements. This also coincided with the maximum displacement before failure occurred (see Fig. 4).

3. In samples 9 through to 14, the failure mode was complete (at 40 kW/m²) or partial loss (at 30 kW/m²) of bond between the laminates from the exposed surface to the mid-thickness. This was accompanied by localised shearing of the laminate due to the force from the loading nose across the mid-thickness (see Fig. 5), however, the maximum displacement before failure appears to be the same regardless of heat flux. By using UHD video the char formation could be properly assessed and appeared to do so at a constant rate. This is due to the rear boundary effectively-being partially a heat sink (steel alloy), which when combined with a constant surface heat flux has been shown elsewhere to experience similar steady-state behaviour using aluminium blocks [22]. The char is also well known in the literature [23] to act as a good natural insulator and hence slow the rate of heat transfer into the material. This appears to be the case during these tests as the temperature distribution data indicate that the char formed, shown with the temperature difference between the exposed and both mid-thickness and unexposed surfaces in Fig. 6b, is around 100 °C. Once ignition occurs the contribution from the flame is notably late in the test as the temperature rises sharply just before failure. Following the tests, these samples were inspected and displayed small quantities of white ash on the exposed surface char layer, indicative of char oxidation. However, the fibres appear largely unaffected, this can be attributed to the pyrolysis of the epoxy resin and subsequent insulator effects of the char formed after this. This shows that the heat fluxes used here were either too low to fully oxidise the char layer and penetrate through to the fibre reinforcement or the exposure time was not long enough.

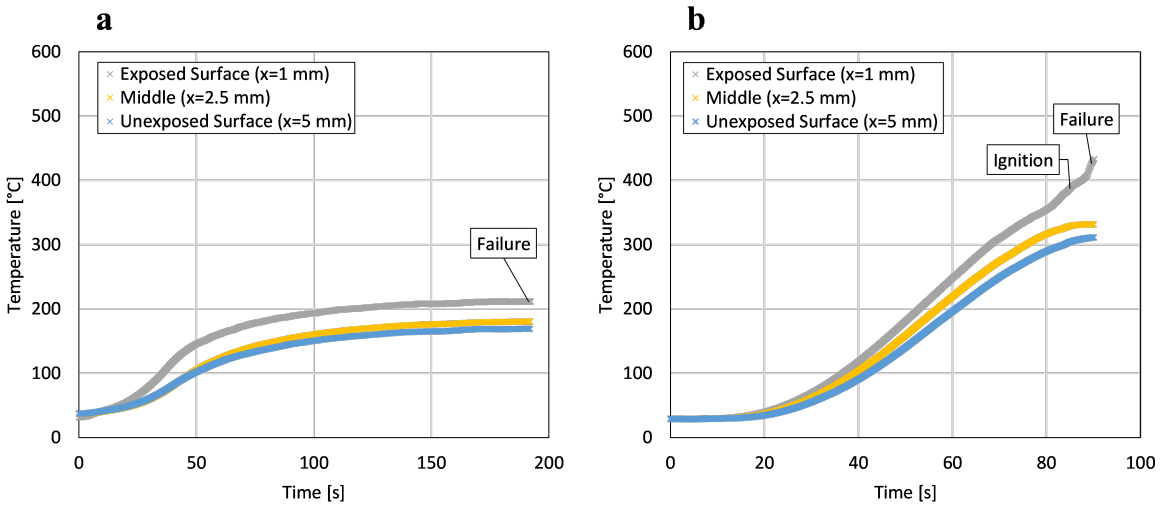

Figure *6* – Time-temperature profiles for a 5 mm thick CFRP material tested at (a) 10 kW/m^2 and (b) 40 kW/m^2.

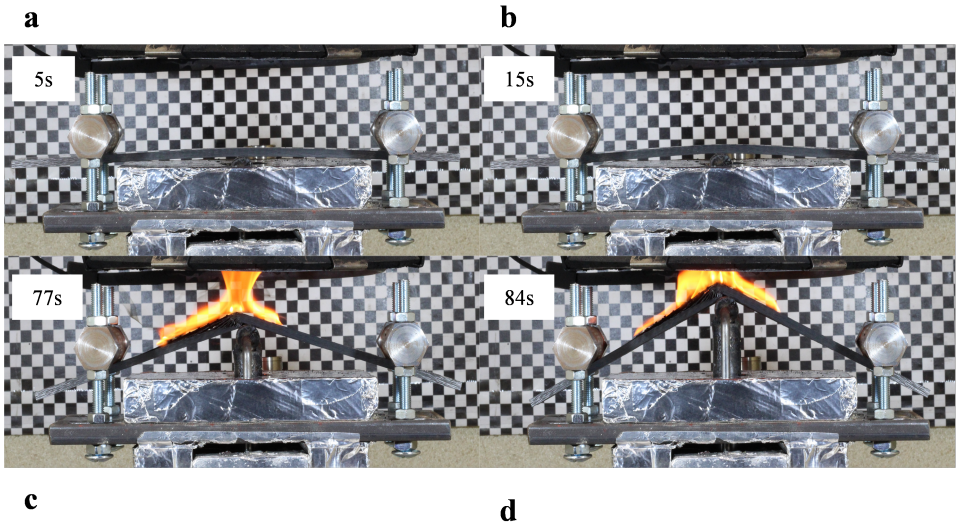

Figure *7* – A snapshot of a sample tested at 40 kW/m^2. Observations show (a) load being applied, (b) beginning of T_g, (c) ignition and (d) failure.

4.3 Time-to-Failure and Failure Modes

Fig. 8 shows the failure modes experienced due to the effects of glass transition at 10 kW/m² (Fig. 8a), and complete loss of bond between laminates at 40 kW/m² (Fig. 8b) to demonstrate the different behaviour of this material depending on heat flux (Table 1 demonstrates the significance of each heat flux relative to fire severity). The failure modes indicate that as heat flux increases the chance of significant delaminations also increases. The tests also show that increasing the heat flux affects the time-to-failure (see Fig. 9) with higher heat fluxes resulting in shorter time-to-failure. At 20 kW/m², the failure time reduces by the largest amount compared to the samples tested at 10 kW/m², however, failure time decreases somewhat proportionally above this value.

In general, the temperature distribution and time-to-failure data suggest that the largest contribution to the failure of CFRP at this thickness is the depth of the glass transition isotherm at 10 kW/m², which has

been shown by the post-fire photographs to have a propensity to induce fibre kinking on the unexposed surface and a loss of bond between the laminates for all the other heat fluxes.

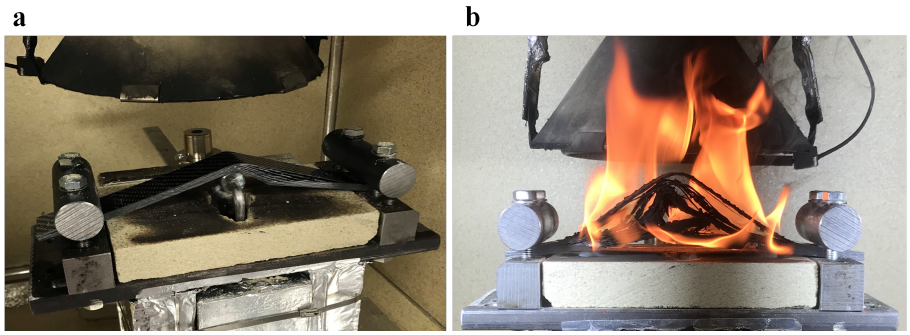

Figure *8* – Images demonstrating the variation of the failure modes with heat flux showing a) T_g induced failure of a sample at 10 kW/m² and b) the sudden failure following ignition at 40 kW/m² showing significant delaminations.

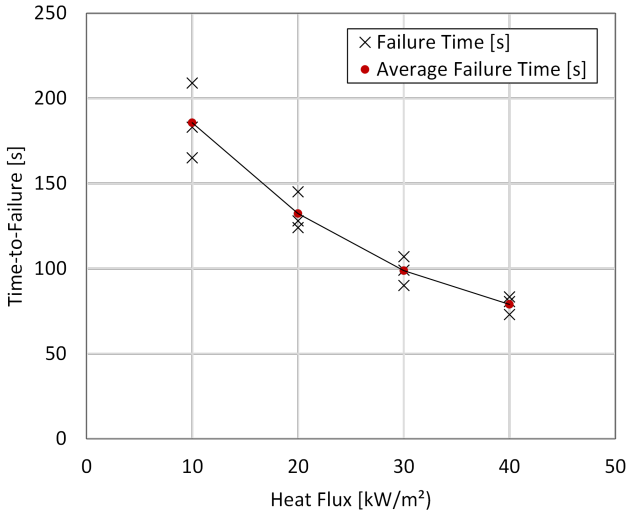

Figure *9* - The time-to-failure of CFRP as a function of heat flux

5 Conclusions

In this paper, a novel testing approach named the ***Thermal and Stress Inducing Device (TSID)*** has been developed and demonstrated to be beneficial in evaluating the three-point bending behaviour of a complex aerospace-grade CFRP material exposed to fire conditions. From this, the following conclusions can be drawn based on the test data briefly described herein:

1. The TSID testing method can quantify the thermomechanical behaviour of a material in a greater level of detail compared to standard post-fire analysis (i.e. separate thermal exposure and bending test).
2. The displacement data revealed that heat flux has little effect on the maximum displacement at the midspan of the samples before failure occurred because at the heat fluxes tested here all the samples had deemed to have failed, however, the time until this failure occurred decreased as heat flux increased.
3. The failure mode is influenced by heat flux. At higher heat fluxes, samples had a tendency to exhibit more brittle behaviour at failure, whilst at lower heat fluxes samples exhibited less brittle behaviour

at failure. The processes that influenced the failure mode include a loss of stiffness leading to fibre kinking on the unexposed surface due to the propagation of the glass transition isotherm through the testing samples. Whilst at higher heat fluxes either a partial or complete loss of bond between the laminates appeared to be the case. In these samples, small quantities of fibre oxidation were also evident in the form of small pockets of white ash..

4. Lastly, the results demonstrated that the TSID can be utilised to accurately assess the coupled interaction between fire conditions and mechanical properties, due to its ability to quantify three-point bending behaviour using heat flux (fire exposure), load-displacement, and time-to-failure data. When failure occurred at higher heat fluxes, the temperature at the exposed surface of the sample was above the glass transition temperature. In most cases, this indicated that although Tg occurs relatively early in the test, (less than 50 seconds), failure occurred much later.

This work, therefore, provides the first step to accurately quantifying the coupled thermomechanical behaviour of CFRP exposed to fire conditions. Ultimately the data generated from this study will allow a better understanding of the role of the material properties (e.g. glass transition temperature, thickness, fibre fraction, resin type) on the performance of CFRP at high temperature to be evaluated and also provide useful input for structural/vulnerability modelling.

Acknowledgements
The authors gratefully acknowledge the financial support for this work from the Defence Science and Technology Laboratory (Dstl).

6 References

[1] A. P. Mouritz, Introduction to aerospace materials, 1st ed. Cambridge: Woodhead Publishing, 2012.
[2] A. Tewarson, "Flammability Characteristics of Fiber Reinforced Composite Materials," 1990.
[3] J. P. Hidalgo, R. Hadden, S. Welch, and P. Pironi, "Effect of Thickness on the Ignition Behavior of Carbon Fibre Composite Materials used in High Pressure Vessels," Eighth Int. Semin. Fire Explos. Hazards, pp. 353–363, 2016, doi: 10.20285/c.sklfs.8thISFEH.036.
[4] A. P. Mouritz, C. P. Gardiner, Z. Mathys, and C. R. Townsend, "Post-Fire Properties of Composites Burnt by Cone Calorimeter and Large-Scale Fire Testing," pp. 1–10, 2008.
[5] C. P. Gardiner, Z. Mathys, and A. P. Mouritz, "Post-fire structural properties of burnt GRP plates," Mar. Struct., vol. 17, no. 1, pp. 53–73, 2004, doi: 10.1016/j.marstruc.2004.03.003.
[6] A. Anjang, V. S. Chevali, B. Y. Lattimer, S. W. Case, S. Feih, and A. P. Mouritz, "Post-fire mechanical properties of sandwich composite structures," Compos. Struct., vol. 132, no. October 2017, pp. 1019–1028, 2015, doi: 10.1016/j.compstruct.2015.07.009.
[7] A. P. Mouritz and Z. Mathys, "Post-fire mechanical properties of marine polymer composites," Compos. Struct., vol. 47, pp. 643–653, 1999, doi: 10.1016/S0263-8223(00)00043-X.
[8] A. P. Mouritz and Z. Mathys, "Post-fire mechanical properties of glass-reinforced polyester composites," Compos. Sci. Technol., vol. 61, no. 4, pp. 475–490, 2001, doi: 10.1016/S0266-3538(00)00204-9.
[9] R. J. Asaro, B. Y. Lattimer, and W. Ramroth, "Structural response of FRP composites during fire," Compos. Struct., vol. 87, no. 4, pp. 382–393, 2009, doi: 10.1016/j.compstruct.2008.02.018.
[10] T. Keller and Y. Bai, "Structural performance of FRP composites in fire," Adv. Struct. Eng., vol. 13, no. 5, pp. 793–804, 2010, doi: 10.1260/1369-4332.13.5.793.
[11] A. P. Mouritz, "Fire resistance of aircraft composite laminates," J. Mater. Sci. Lett., vol. 22, no. 21, pp. 1507–1509, 2003, doi: 10.1023/A:1026103231041.
[12] A. . Mouritz and A. G. Gibson, Fire Properties of Polymer Composite Materials, 1st ed. Dordrecht: Springer, 2006.
[13] J. G. Quintiere, Fundamentals of Fire Phenomena, 1st ed. College Park: John Wiley & Sons, 2006.
[14] S. Feih and A. P. Mouritz, "Tensile properties of carbon fibres and carbon fibre-polymer composites in fire," Compos. Part A Appl. Sci. Manuf., vol. 43, no. 5, pp. 765–772, 2012, doi: 10.1016/j.compositesa.2011.06.016.
[15] S. Feih, Z. Mathys, A. G. Gibson, and A. P. Mouritz, "Modelling the tension and compression

strengths of polymer laminates in fire," Compos. Sci. Technol., vol. 67, no. 3–4, pp. 551–564, 2007, doi: 10.1016/j.compscitech.2006.07.038.
[16] D. Swanson and J. Wolfrum, "Time to failure modeling of carbon fiber reinforced polymer composites subject to simultaneous tension and one-sided heat flux," J. Compos. Mater., vol. 52, no. 18, pp. 2503–2514, 2018, doi: 10.1177/0021998317749711.
[17] D. Swanson and J. Wolfrum, "Effects of simultaneous compression and one-sided heat flux on the time to failure of carbon fiber-reinforced polymer composites," J. Compos. Mater., vol. 52, no. 13, pp. 1809–1819, 2018, doi: 10.1177/0021998317734392.
[18] L. A. Burns, S. Feih, and A. P. Mouritz, "Compression failure of carbon fiber-epoxy laminates in fire," J. Aircr., vol. 47, no. 2, pp. 528–533, 2010, doi: 10.2514/1.45065.
[19] A. P. Mouritz, "Post-fire flexural properties of fibre-reinforced polyester, epoxy and phenolic composites," J. Mater. Sci., vol. 37, no. 7, pp. 1377–1386, 2002, doi: 10.1023/A:1014520628915.
[20] A. . Mouritz, Z. Mathys, and C. . Gardiner, "Thermomechanical modelling the fire properties of fibre–polymer composites," Compos. Part B Eng., vol. 35, no. 6–8, pp. 467–474, 2004, doi: 10.1016/j.compositesb.2003.09.005.
[21] M. A. Delichatsios, "Turbulent Convective Flows and Burning on Vertical Walls," Ninet. Symp. Combust. Combust. Inst., pp. 855–868, 1982.
[22] A. Ito and T. Kashiwagi, "Characterization of Flame Spread over PMMA Using Holographic Interferometry Sample Orientation Effects*," Combust. Flame, vol. 204, pp. 189–204, 1988.
[23] J. P. Hidalgo, P. Pironi, R. M. Hadden, and S. Welch, "Experimental study of the burning behaviour of a commercial carbon fibre composite material used in high pressure vessels," ECCM 2016 - Proceeding 17th Eur. Conf. Compos. Mater., no. June, pp. 26–30, 2016.
[24] Society of Fire Protection Engineers, SFPE Handbook of Fire Protection Engineering, 5th ed. Springer, 2016.